Exoplanet Direct Imaging with the Palomar Vortex Coronagraph

Rahul I. Patel[1], Stanimir Metchev[1]

[1]Department of Physics and Astronomy at Stony Brook University

Abstract

We present projections for the planet detection rates from a survey for Jovian type exoplanets orbiting young, nearby targets. We will be using the novel **Palomar vortex coronagraph** (**PVC**; Mawet et al. 2010) , in conjunction with **PALM-3000** extreme adaptive optics (ExAO) system. PALM-3000 employs a 3366 - actuator deformable mirror and is expected to deliver contrast ratios near 10^7 at 1 arc second from bright stars. The PALM-3000 system is an upgrade from the current adaptive optics system at Palomar and commissioning will begin in the summer of 2011. We explore the sensitivity of the PALM3000 & PVC system through Monte-Carlo simulations of planets in a range of orbits and masses. Projected contrast curves in the *H* band for the PVC were used as the constraints for planetary detection. Planetary and orbital parameters (mass, eccentricity, semi-major axis) were randomly sampled from known distributions (Cumming et al. 2008), which have been established or extrapolated from radial velocity observations. Host stars were modeled in accordance with the stellar initial mass function (IMF; Kroupa 2001), given uniformly distributed random ages and set at random locations within a 100 pc radius volume around the sun.

Inputs for Planet Detectability Simulations

1. Simulate Universe

Stars were randomly generated:

- Following Kroupa (2001) IMF
- Stellar Density: 0.1 stars $(pc)^{-3}$
- Stellar Mass distribution (0.5 – 7.0 $M_{\odot}$)
- Distances < 100 pc.
- Ages from 1 Myr to 10 Gyr.
- Luminosities from:
  - **Pre-Main Sequence**: Evolutionary models of Siess et al. (2000)
  - **Main Sequence**: Mass → T_{eff} → Luminosity empirical relations.

2. Simulate Planet Population

- A single planet generated around each star
- Orbital semi-major axes and eccentricities selected at random from distributions in Table 1
- Uniformly random orbital orientations
- Planet Luminosities derived from CONDO3 Hot Start models (Baraffe et al. 2003)

Parameter	Distribution	Range
Planet Mass	$\frac{dN}{dq} \propto q^{-1.31}; q = \frac{M_p}{M_s}$	0.5 – 12 M_J
Eccentricity	$\frac{dN}{de} \propto e^{-0.5}$	0.0 – 0.8
Semi-Major Axis	$\frac{dN}{da} \propto a^{-0.61}$	0.1 – 75 AU

Table 1. Planetary and orbital distributions used in simulations. SMA distribution extracted from Cumming et al. (2008).

3. Detecting Planets

- Only stars with H ≤ 5 mag were selected for this simulated survey
- Detection of a planet is dependent on:
  - Planet to star contrast in the H band being above the projected 5σ sensitivity limit for 1 hour integrations.
  - Planet angular separation falling between 0.067 – 3.0 " for PVC. The outer working angle for PVC has been set somewhat arbitrarily to avoid significant contamination from background stars.
- Comparison Monte-Carlo with Gemini Planet Imager (GPI) was also performed.
  - The inner and outer working angles for GPI were set to correspond to the 0.142 – 1.17" highest contrast region

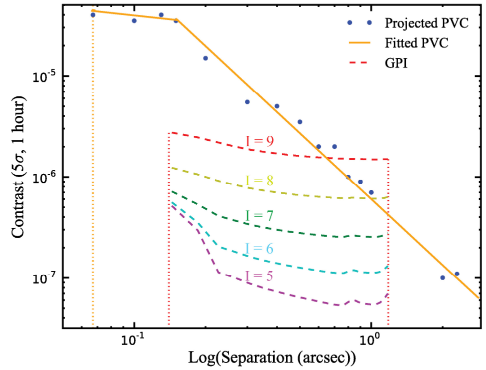

Fig 1 - Preliminary projected contrast curves in the *H* band as a function of angular separation for both the Palomar Vortex Coronagraph (Serabyn 2010) and the Gemini Planet Imager. The curves are based on a 5σ sensitivity limit for 1 hour integrations on a given target. The PVC curve was taken on a H = 5 mag star and depicts the performance expected in the first phase of observations. The GPI curves were taken from I = 5 to I = 9 mag. For VVC, actual contrast data on the test star is depicted by the blue data points. Two linear functions were fit to these data (orange) in order to facilitate use of the contrast curve for planet selection. The vertical dotted lines depict the adopted inner and outer working angle (IWA, OWA) of each instrument (PVC → [0.067:3.0], GPI→ [0.142:1.17] arc seconds).

Planet Detection Rates

Palomar Vortex Coronagraph

Fig. 2 – The fraction of detected planets among all the planets simulated in a given bin is plotted for the PVC. The column of panels plots the fractional detection of planets for a given planet mass or planetary separation. The rows depict three different age and volume limits for surveys – the same as in McBride et al. (2010). Detection probability is plotted for a given spectral type of the host star, along with an average detection (for all simulated stars) in each survey. The planet masses generated in these surveys are set by the planet-to-star mass ratio distribution (dN/dq) as shown in table 1. Only stars with H band magnitude ≤ 5 are used in these surveys.

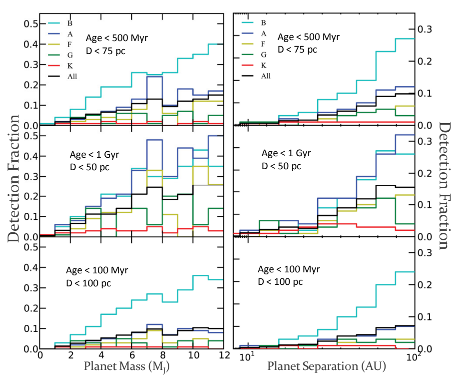

Fig. 3 The fraction of detected planets among all the planets simulated in a given bin is plotted for the PVC. The sub-samples plotted in each panel are the same as in Fig. 3. Results are listed for planets detected around all the targets for each survey. The red and blue lines distinguish whether the generated planet mass is dependent on its host mass (dN/dq; as proposed in McBride et (2010)) or not (dN/dM_p) respectively. For planet masses generated independently of the host star mass, the adopted parent planet mass distribution follows an $M_p^{-1.31}$ power law, as for the mass ratio distribution (Table 1). Again, only stars with H band magnitude ≤ 5 are used in these surveys.

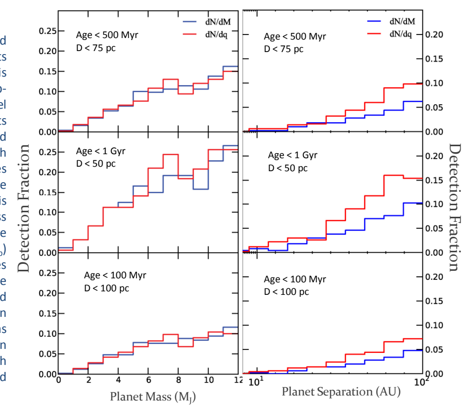

Gemini Planet Imager

Fig. 4 – Simulations of the planet detection efficiency of GPI under identical assumptions as for the PVC. The distribution for planetary separations of planets detected with GPI is consistent with similar simulations performed in McBride et al. (2011). The shape of the distribution for planet masses is similar to McBride et al., yet slightly inflated. This may be due to the selection of only bright stars for all surveys. Compared with PVC (Fig. 2), the planet detection efficiency of GPI is poorer at <8 AU and greater t >40 AU, and superior within this orbital range.

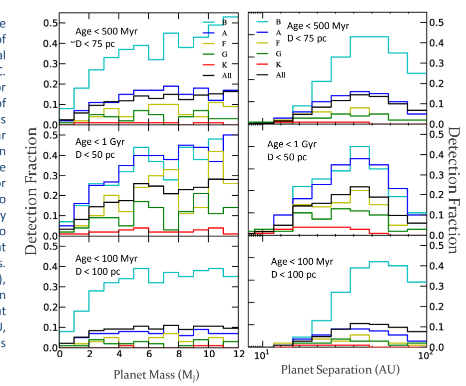

Conclusions

From these simulations, the probability of detecting a planet is seen to increase with planet mass. The highest detection rates (>20%) are found around the brightest host stars at larger separations (>40 AU). The fraction of detected planets increases with separation, as opposed to the simulation results from the GPI coronagraph, where the yield decreases past ~ 40 AU compared to that of GPI. This is mainly due to the larger OWA angle of PVC compared to that of GPI's. There's also a significant number of detections at close separations – down to 4-5 AU for the closes stars (given the statistical sample of the solar neighborhood) which are not seen for GPI.

For nearby young stars (<75 pc), detection rates >10% are seen for M_p > 6-8 M_J, out to ~20 AU. For nearby stars in general, detection rates > 10% are seen for M_p > 4-5 M_J out to ~ 10-12 AU. Further out, detection rates drop except for the earliest type stars for both PVC and GPI.

Future Work

- Compile viable target list
- Awarded time at Palomar for observations in 2012
- Imaging using PHARO near-IR camera in *H* band

References

Baraffe, I., et al. A&A, 402, 701
Kroupa, P. 2001 MNRAS, 322, 321
Serabyn, E. 2010, Private communication.
Beichman, C.A., et al. 2010, PASP, 162, 200
Mawet et al., 2010, ApJ, 709,53
Siess L., Dufour E., Forestini M. 2000, A&A, 358, 593-599
Cumming, A., et al. 2008, PASP, 120, 531
McBride, J., et al. 2011